Provisional report of the geotechnical risks caused by the Mw=7.8 Nepal earthquake of April 25, 2015[1]

By

Kazuo KONAGAI, Dr. Eng., Leader, Professor, Yokohama National University.

Rama Mohan POKHREL, PhD, JSPS Research Fellow, IIS, University of Tokyo.

Hitoshi MATSUBARA, Dr. Eng., Assistant Prof., University of the Ryukyus, and

Masataka SHIGA, Undergraduate Student, Yokohama National University.

Preface

The April 2015 Nepal earthquake of Mw=7.8, also known as the Gorkha earthquake, was the worst natural disaster to strike Nepal since the 1934 Nepal–Bihar earthquake. As of May 26th, the police report had confirmed 8,664 fatalities, with more than 21,954 injured (Source: Japan Embassy in Nepal). The quake was followed by many aftershocks including the one of M=7.3 that struck north-eastern Nepal on Tuesday, May 12th. Among the areas of most concern are those where soil/rock masses detached from slopes have fallen into rivers, posing an ongoing menace that will be likely to increase when seasonal monsoon rains begin to fall in June. This report outlines the findings obtained through the reconnaissance of the JSCE Landslide survey group, JSCE/JGS/JAEE joint Investigation Team for the 2015 Nepal Earthquake Disaster. Some descriptions in this report are not fully evidenced yet, and therefore, some comments are not yet the conclusions reached after a thorough discussions among the members. However, providing both Japan and Nepali experts and persons in charge with a rough-an-ready overview will be important for taking measures for the disaster relief and rational rehabilitations.

Locations of landslides

"Landslides triggered by the 25 April Nepal earthquake were mapped by experts at the British Geological Survey, Durham University, and a volunteer group coordinated by NASA-JPL, the University of Arizona, and ICIMOD, and are provided in the ArcGIS geodatabase format on the following webpage[1], [2]:
https://data.hdx.rwlabs.org/dataset?q=Nepal+earthquake+landslide+locations%2C+8+May+2015.
Satellite data used to prepare this data set include those from the International Charter Space and Major Disasters, as well as freely-available online viewers. Maps for our survey were prepared given this set of digital data (Fig. 1). Note that the dataset was last updated on May 8th, 4 days before the largest Mw=7.3 aftershock of May 12.

---

1 Tentative version of June 1st, 2015, 3rd revision on June 9th, 2015.

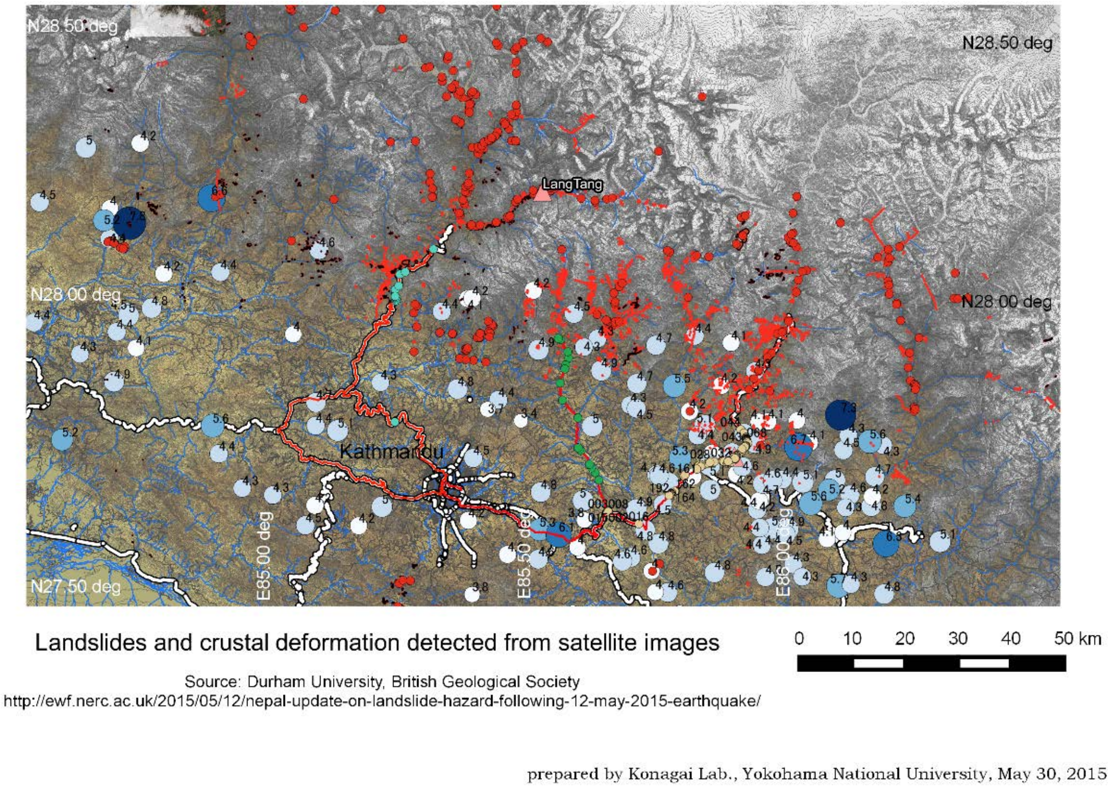

Fig. 1 Prepared map of landslides and aftershocks

(Landslides location data from the British Geological Survey, Durham University [1], [2])

Discharge

Since one of the major post-quake concerns is the increase in discharge of river water in the upcoming rainy season, a rough and ready estimation of peak discharges was made at 2 points along the Sunkoshi River (Table 1).

Table 1. Locations of chosen points

Point Number	Longitude	Latitude
1	E85.88150°	N27.81655°
2	E85.82750°	N27.75387°

River water depth h is first estimated by observing hydraulic disturbances transmitted downstream within a steady cone of apex angle θ (Fig. 2)

$$v_{jump} = \sqrt{gh} = v_{flow}.\sin\theta$$

where, $g =$ gravitational acceleration, and $v_{flow} =$ observed flow velocity.

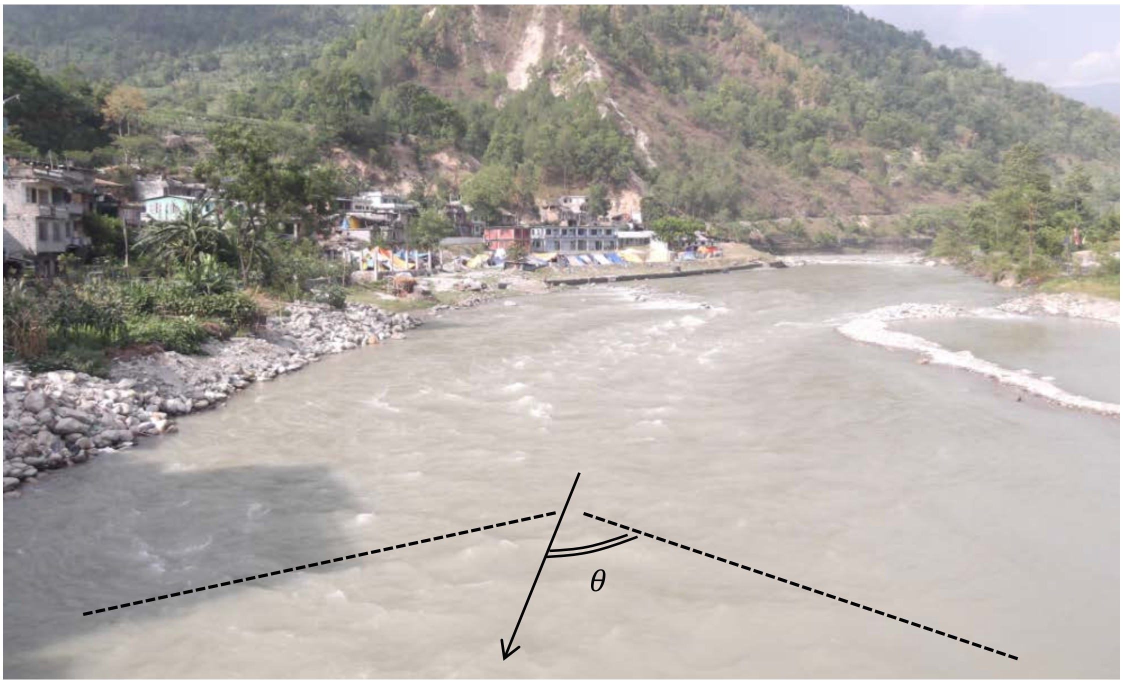

Fig. 2 Hydraulic jump propagating across flow at an angle θ at Point 2 (N27.75387°, E85.82750°)

Table 2 Manning's roughness coefficients n estimated at two points along Sun Koshi river

Point No.	Observed flow velocty (m/s)	Angle at which wave propagates across flow (deg)	Velocity of Hydraulic jump (m/s)	Estimated maximum depth (m)	River bed drop (m)	over Distance (m)	River bed inclination	Hydraulic radius (m)	Average flow velocity (m/s)	Estimated Gauckler–Manning coefficient
	v_{flow}	θ	$v_{jump} = v_{flow}.\sin\theta$	$D_{max} = {v_{jump}}^2/g$	Δh	L	$i = \Delta h/L$	$R \cong 2 \times D_{max}/3$	$v_{ave} \cong 2 \times v_{flow}/3$	$n = R^{2/3} i^{1/2}/v_{ave}$
1	3	45	2.12132034	0.459184	5	128.6	0.0388802	0.30612245	2	0.044781432
2	2.9	70	2.7251086	0.757777	4.6	232.4	0.0197935	0.50518482	1.93333333	0.046158779

Manning's empirical equation is then used to calculate Manning coefficient of roughness n at the chosen points:

$$v_{ave} = \frac{1}{n} R^{2/3} i^{1/2}$$

where $v_{ave} =$ cross-sectional average velocity (m/s) which is tentatively assumed to be 2/3 of the observed peak flow velocity v_{flow}, $R =$ hydraulic radius (m) and $i =$ slope of the hydraulic grade line. Though it may be a mere coincidence that the estimated roughness coefficient values n are about the same with each other, these values lie in ranges recommended by the Japan Ministry of Land, Infrastructure, Transport and Tourism (MLIT) for mountain river beds covered up with gravel ($0.030 < n < 0.050$) and big boulders ($0.040 < n$). Therefore the average value of $n = 0.045$ is used to estimate both current and peak discharges. To estimate peak discharges, the peak water depths are estimated based on eyewitness accounts (Table 3).

Table 3 Estimated current (May 28, 2015) and peak discharges (m^3/s)

Point No.	Effective river water width (m)	water cross-section (m^2)	Current discharge	Credible increase of river water level (m)	Increase in river width (m)	Credible maximum river-water cross section	Credible peak velocity	Credible peak discharge
		$A \cong W \times D_{max}/2$	$Q_{current} \cong v_{ave} \times A$					
1	30	6.887755102	13.7755102	2	2	73.79591837	7.685783	567.17942
2	28	10.60888126	20.5105038	2	20	120.2488715	5.622115	676.05298

Peak average velocities of 7.7 to 5.6 m/s associated with the estimated peak discharges of 500 to 700 m^3/s may occur in the rainy season, which velocities can be substantially large for the river-bed load including large boulders to be eroded as can be predicted by the curve shown in Fig. 3[2].

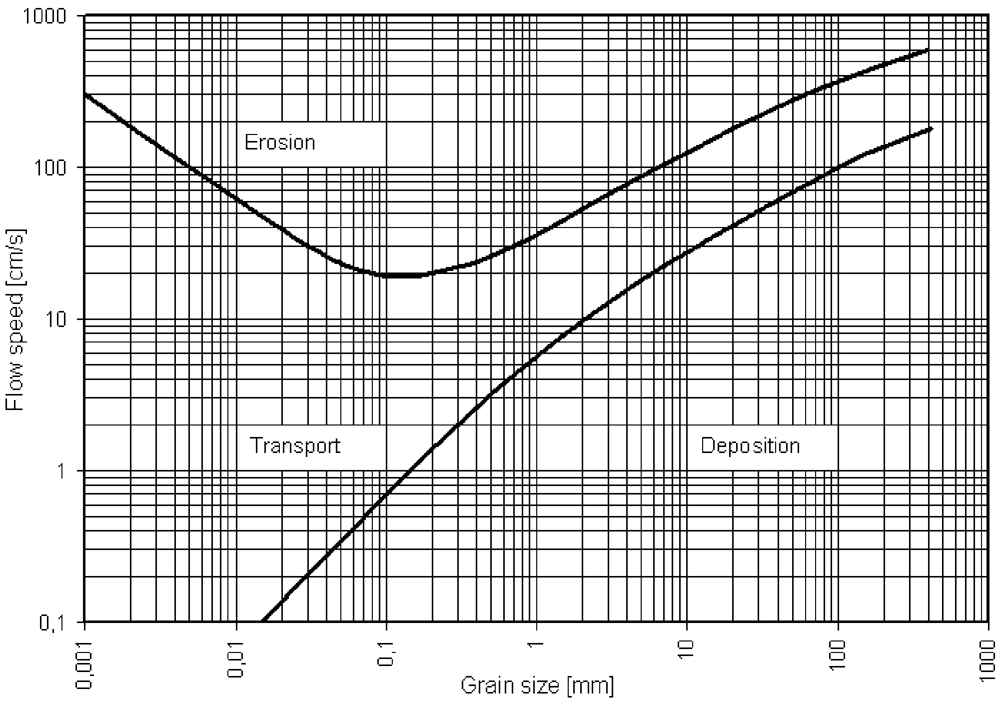

Fig. 3 Hjulström curve showing the critical current velocity required to move grains on a plane bed

[2] Note that this Hjulström-Sundborg Diagram has no more than a historical value nowadays (Wikipedia), although its simplicity is still attractive, and currently more rational approaches are taken to estimate river bed load transport. The rate of riverbed load transport is to be discussed given much more precise pieces of information to cope with problems for intake facilities of hydropower stations, etc.

Sunkoshi Landslide

Heavy rainfall on August 2, 2014 triggered a landslide on a steep valley wall of metamorphic rock of Sunkoshi river. The landslide mass reportedly killed 156 people and blocked the river to form a lake behind it. Though the landslide was not caused by the earthquake, the presence of the landslide mass that has fallen in the river will certainly have an important and serious effect on the riverbed load transport and thus important facilities such as intake gates for hydropower stations. It is reported by the Earth Observatory, NASA that some 5.5 million cubic meters of rock and debris tumbled down into the Sunkoshi River valley[3]. A 3D image of the exposed slip surface was made to see more details of detached and deposited rock and debris using Epipolar geometry[4], which geometry allows a 3D image from photos taken from different locations to be reconstructed. Though three photos were taken from three different Points 1, 2 and 3 (Table 3), Points 2 and 3 are very close to each other. Therefore one more reference point (Point 4) was taken for much better control of positioning at an exposed rock on the intact mountain slope, which can be seen from all the camera locations. The longitude, latitude and elevation of this point were tentatively obtained from a Landsat imagery and the 30m SRTM DEM[5].

Fig. 4 Sunkoshi Landslide

(Photo by K. Konagai taken at N27.761312, E85.875274, on May 28th, 2015)

Table 3 Reference points for reconstructing 3D image

Point No.	Longitude (degree)	Latitude (degree)	UTM value easting, *x* (m)	UTM value northing, *y* (m)	Elevation (m)
1	85.869678	27.755511	388609.86	3070631.27	896.535034
2	85.876536	27.76144	389291.83	3071281.94	893.824341
3*	85.875274	27.761312	389167.33	3071268.88	864.986816
4	85.869813	27.772017	388640	3072460	1380

* Coordinates of Point 3 were not used for geo-referencing.

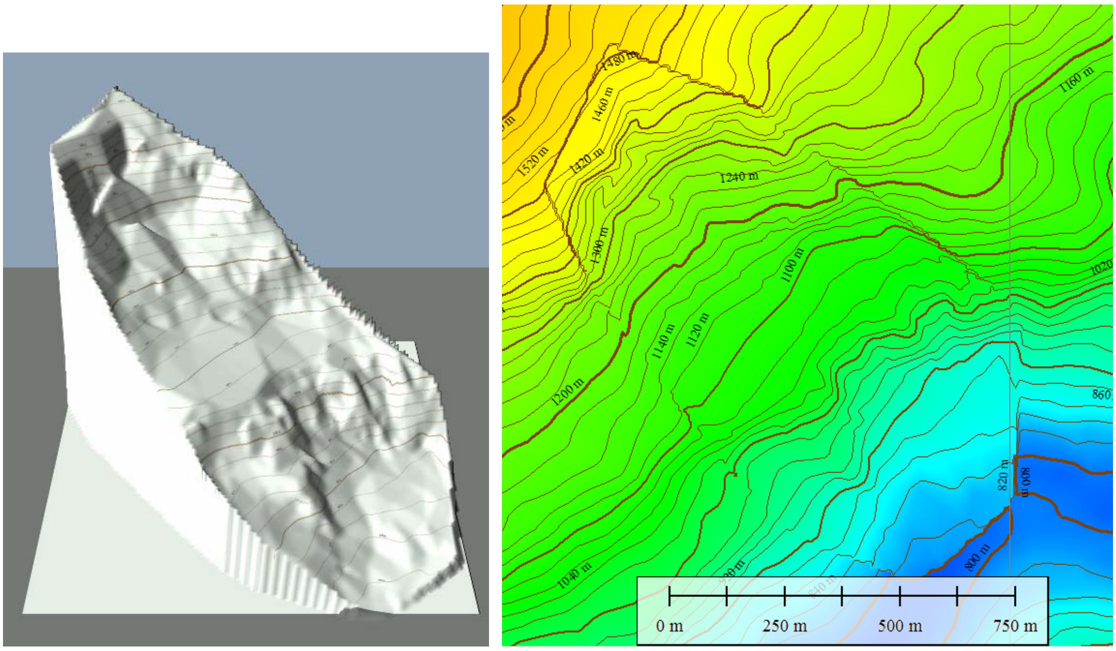

Fig. 5 DEM of slip surface of Sunkoshi Landslide

The obtained digital elevation model for the exposed slip surface of Sunkoshi is shown in Fig. 5. Though the entire stretch of the exposed surface was not completely covered, there are a clear hollow of the top source region, major triple-terraced cliffs on the top, halfway up and near the toe of the exposed surface with conic talus deposits (collections of broken rock fragments) rimming along the bases of these cliffs. The angle of repose for these talus deposits varies from 15 for low-lying coarse rock deposits to 30 degrees for high-lying finer granular deposits.

A 30m SRTM digital elevation model[5] was used herein as the terrain model before the landslide event, and compared with the obtained digital elevation model of the exposed slip surface. Fig. 6 shows the change in elevation within the measured slip surface area.

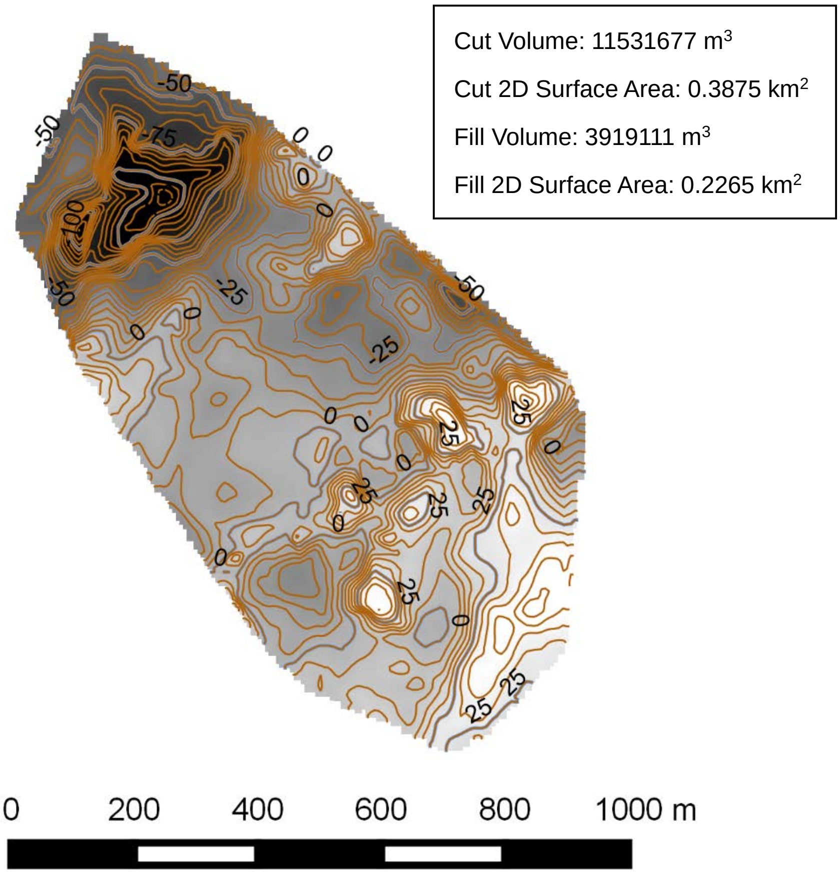

Fig. 6 Change in elevations within the exposed slip surface

The volumes of the detached and deposited masses are estimated to be 11.6 million m^3 and 3.9 m^3 respectively. The observed area is not covering the major part of the soil mass that has fallen into the river, and the remaining mass of 7.7 million m^3 may be as much as the rock/debris volume of 5.5 million m^3 estimated by NASA[3]. However, the estimated volumes are sensitive to points taken for geo-referencing (Table 3), and revised values will be reported in the updated version of our report.

Creeping landslide mass

According to eyewitness accounts, an about 1.5 km long soil mass was first detached in the heavy rain season of 2002 from the zone of about 2100m ASL on a high mountain slope, and fell along a deeply incised gulley down to Trishuli river about 1300m below the exposed scar to clog the stream. A temporary road was quickly constructed across this zone for the important traffic of Trishuli road leading to Dhunche not to be suspended long.

However, the road started moving inch by inch towards the toe. Fig. 7 shows two satellite images of the zone from different times, the upper and lower ones from May 3, 2015 and January 4, 2010, respectively. It is noted in the latest 2015 photo that the temporary road section crossing the landslide zone is currently west of the location where this section used to be in 2010, indicating that this section has been carried down the slope over about 30m horizontal distance. Moreover swaths of bare slip surfaces above the temporary road, which swaths were not visible in the 2010 photo, are appearing and becoming thicker year by year. Though the earthquake had reportedly invisible and indirect effect upon the remaining landslide mass, the movement of the mass can be further accelerated in the upcoming rainy season of 2015.

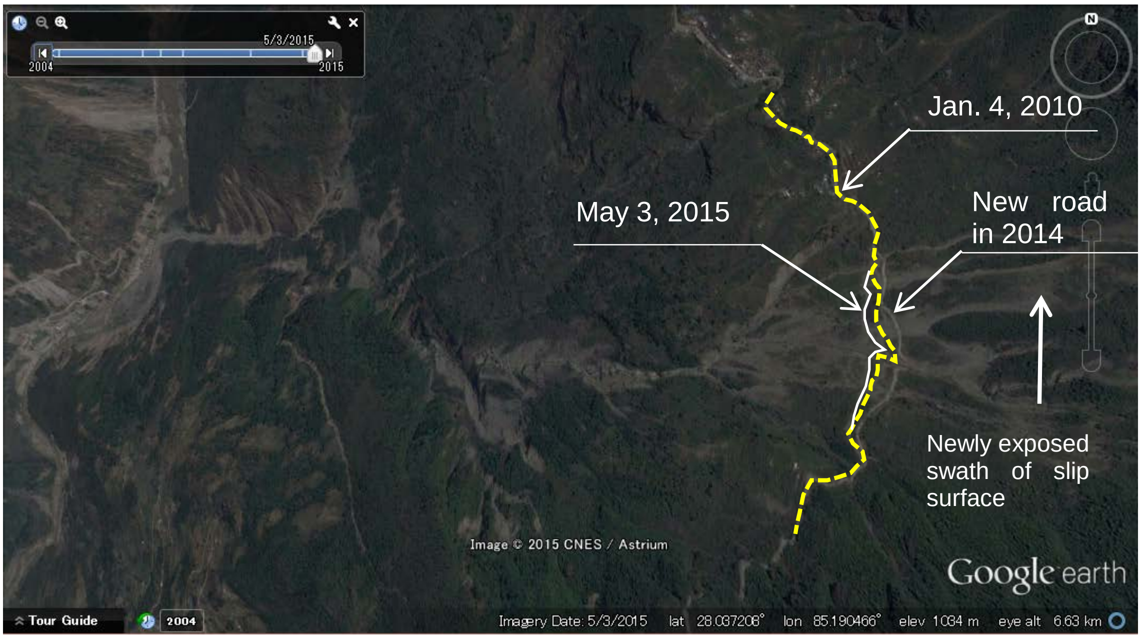

(a) Landslide zone on May 3rd, 2015

(b) Landslide zone on January 4th, 2010

Fig. 7 Landslide zone (Satellite images taken from Google Earth)

Fig. 8 Sign of dilating debris mass halfway up on a landslide mass, which was cut at this elevation for the temporary road construction at N28.067959°, E85.228808°

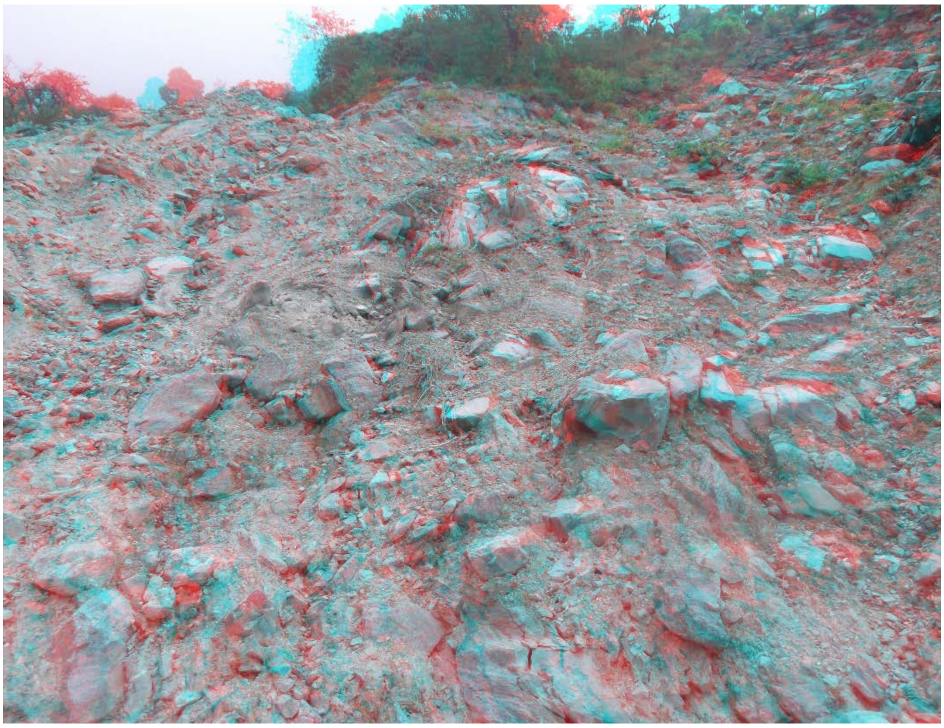

Fig. 9 3D stereoscopic visualization of the sign of dilating debris mass
at N28.067959°, E85.228808°
(3D red cyan glasses are recommended to view this image correctly)

All along the Trishuli road from this point of continuous creeping to Dhunche, clear indications of dilating landslide masses can be seen from place to place. Fig. 8 shows a pair of photographs of a dilating debris mass halfway up on a landslide mass, which was cut at this elevation for the temporary road construction. These photos, arranged side by side can be perceived as a single image in terms of depth, and one notices that the matrix of fine sand filling up the voids of sub-angular rocks/ boulders exhibits fresh open cracks, an indication that the fabric of these embedded large rocks are slowly dilating. An anaglyph 3D image of this debris mass is shown in Fig. 9.

Depressed section of Araniko Highway

Several lines of vertical ground dislocations appeared diagonally across Araniko highway making up a 200m wide swath of ground failure. Way points are marked along visible dislocation lines by a GPS receiver as shown in Fig. 10. The observed ground dislocation lines are about parallel to each other trending in NEE to SWW direction curved slightly north. These lines die out beyond their eastern and western ends, and about 300 to 400 m long at the most, indicating that the failure was just localized within this short extent of the swath. Two outermost lines of relatively large dislocation indicates that the area between these two major dislocation lines has sunken by about 2m.

However the inner-most lines suggest that the lowest wet zone may have been pushed slightly up. To highlight this feature of mass movement, a longitudinal section of the highway was measured by using a handy laser-ranger (Fig. 10).

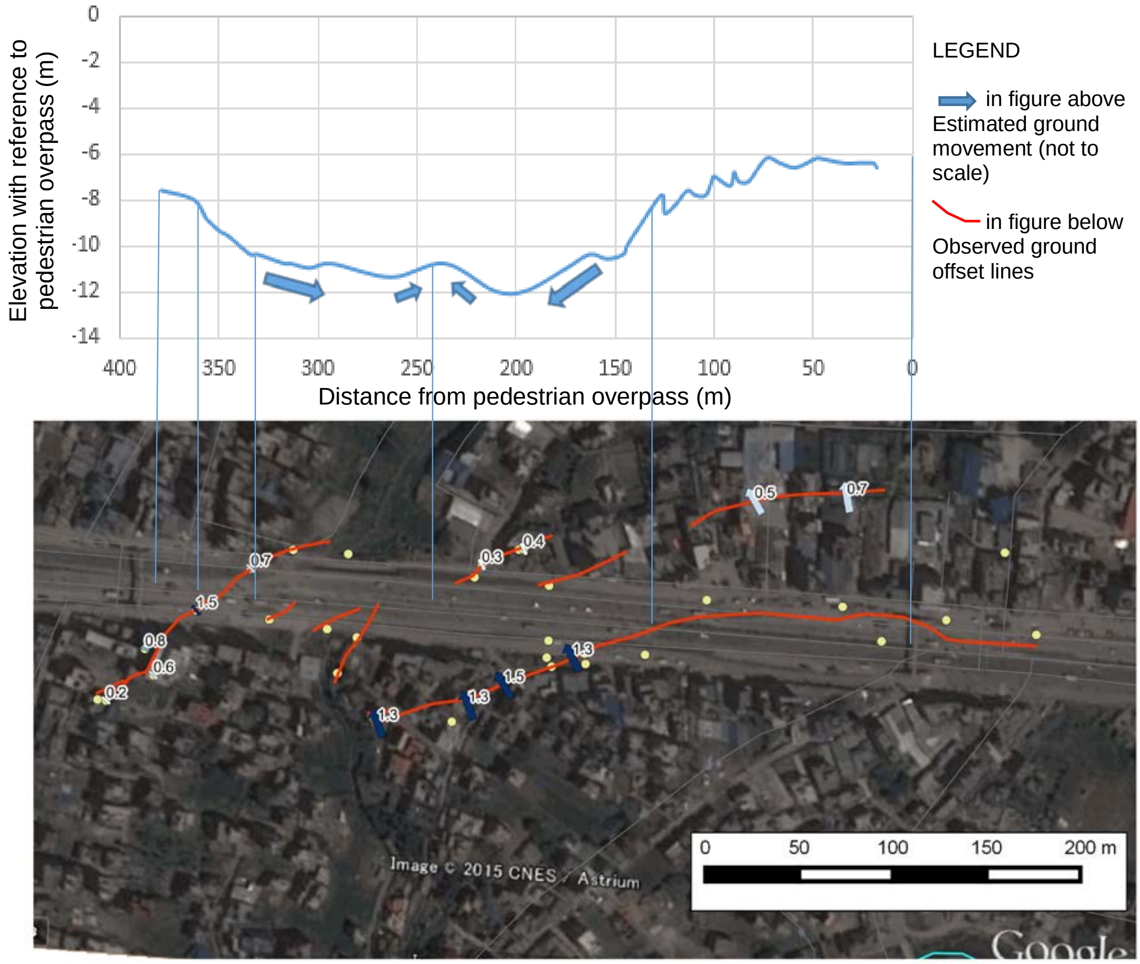

Fig. 10 Depressed section of Araniko Highway and ground offsets (Photo from Google Earth)

Though the cause of this ground depression is yet controversial, the authors think that a local lateral spread of sandy hill slopes towards the low-lying wet ground was responsible for this failure. The wet and slightly depressed area along a small canal may have been liquefied and/or weakened enough to allow the sandy hillsides on both sides of the canal to move a little sideways against each other, and bulged. This ground depression was responsible for the deformation of a two-span continuous pedestrian overpasses, whose north pier rests exactly on the south-easternmost line of dislocation while the other two are on the relatively intact hill terrace. As the result, the northern pier was on an outward tilt, causing the joint between the pier and the deck to open up by about 40 to 45 cm. It was lucky that the deck of the overpass did not fall onto the highway probably because it was a two-span continuous beam. However there could have been a good chance for any single supported deck of overpass to fall upon the highway with its spans expanded. According to one of our members who have been there on May 2nd, the joint may have been opened a little wider (Fig. 11), indicating that the tilt of the pier has been increasing gradually and/or in a step-wise manner over a month's period since the earthquake hit.

Fig. 11 Joint opened between deck and pier of the pedestrian overpass. Photos left and right by R. Pokhrel on May 2nd and 31st, 2015, respectively, at N27.674601°, E85.364705°: Assuming that the notch depth *D* of the pier-top landing for the bridge-girder seating is the same for both photos of May 2nd and May 31st, these photos are suggestive that the joint has opened a little wider over a month's period.

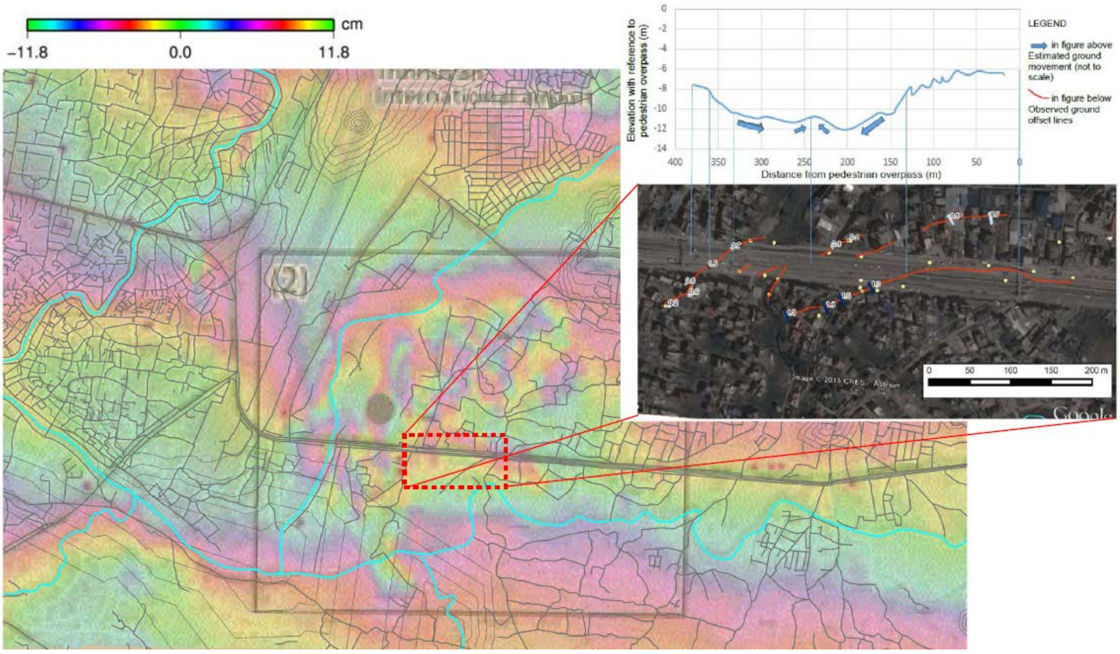

Fig. 12 Disturbance of InSAR fringe pattern near sagging section of Araniko Highway (PALSAR-2 InSAR from [6])

Given the above findings, local soil conditions are to be carefully reflected upon rehabilitation plans in a rational manner, because as has been frequently seen in the past earthquakes, it can take months for liquefied/weakened soil to regain its initial strength, and even after it regains the strength, the soil can remain susceptible to re-liquefaction in a next big earthquake. To pinpointing locations of weak soils, InSAR imageries may be useful as shown in Fig. 12 which figure exhibits disturbance of enlarged PALSAR-2 InSAR fringe pattern near the depressed section of the highway.

Necessary measures/ recommendations

(1) Continuously moving mountain slopes:

Continuous monitoring of creeping slopes from satellites is important. Once early signs of accelerated movements are found, pin-point countermeasures for villages and roads can be taken in a quick and rational manner.

(2) Debris/ riverbed load transportations:

Peak discharge and associated riverbed load transportation rate are to be estimated based upon much more reliable information. This estimation is particularly important to deal with potential risks for intake facilities of hydropower stations, etc.

(3) Landslide masses clogging streams

Volumes and dimensions of large landslide masses clogging major streams are also to be estimated.

(4) Depressed section of Araniko Highway

Something that should not be forgotten in discussing rehabilitation strategies is that a large earthquake often causes long lasting geotechnical problems. Once liquefied, soil can remain soft for months. Locations with similar land deformations to the depressed section of Araniko Highway are to be identified and their causes are to be thoroughly studied to reflect the natures of weak soils upon rehabilitation/ reconstruction plans.

Acknowledgement

Special thanks of the authors go to Mr. Masashi Ogawa, Ambassador, Mr. Shinya Machida, Counsellor, and Mr. Makoto Oyama, First Secretary at the Embassy of Japan, Kathmandu, Nepal, who have provided the authors with briefing of the earthquake-induced damage, and organized an information exchange meeting among Japanese reconnaissance teams.

References:

[1] Durham University / BGS Team, Nepal earthquake landslide locations, 8 May 2015,
https://data.hdx.rwlabs.org/dataset/lands
https://data.hdx.rwlabs.org/dataset?q=Nepal+earthquake+landslide+locations%2C+8+May+2015

[2] Durham / BGS Team, Nepal: UPDATED (28 May) landslide inventory following 25 April Nepal earthquake, etc., http://ewf.nerc.ac.uk/blog/

[3] NASA Earth Observatory, Before and After the Sunkosi Landslide,
http://earthobservatory.nasa.gov/NaturalHazards/view.php?id=84406

[4] SolidFromPhoto 32
http://www.solidfromphoto.sakura.ne.jp/

[5] The humanitarian Data Exchange, Central Nepal Digital Elevation Model (DEM),
https://data.hdx.rwlabs.org/dataset/9cdbade9-fca2-4d23-99ab-9f3a396ae929/resource/f895e259-17da-4973-a8fb-97f8628e8e63

[6] Earth Observation Research Center, Japan Aerospace Exploration Agency, ALOS-2/PALSAR-2 Observation Results of the 2015 Nepal Earthquake (4),
http://www.eorc.jaxa.jp/ALOS-2/en/img_up/dis_pal2_npl-eq_20150502.htm